UNIVERSITY OF CALIFORNIA,
IRVINE

# Cellular Crosslinking of *B. subtilis* via Conjugation of Polymerizable Handles

THESIS

submitted in partial satisfaction of the requirements
for the degree of

MASTER OF SCIENCE

in Biomedical Engineering

by

Wesley Alan Groves

Thesis Committee:
Assistant Professor Seunghyun Sim, Chair
Associate Professor Jered Haun
Assistant Professor Tim Downing

2022

# TABLE OF CONTENTS

# LIST OF FIGURES

# ACKNOWLEDGEMENTS

I would like to acknowledge the contribution of my committee chair, Seu Sim, for the continued support and scientific guidance. I would also like to thank the fellow Sim lab member Esteban Bautista-Garcia for his friendship, emotional support, and chemistry tutoring sessions. Sim lab post-doc Hyuna Jo deserves acknowledgment for being a beacon of light, whose scientific prowess and grit is an inspiration to all around her. I need to acknowledge my lifelong best friend, Jenn Urbine, who has had tremendous positive influence on my life and is one of the reasons I found a passion for science. My partner, Parker, deserves acknowledgement for being a continuous source of love and support throughout my entire time in graduate school.

Lastly, and most importantly, I want to thank my parents for always supporting me as I find my own path through life. Without them, I wouldn't be who I am today. I hope to use the life they gave me to leave a positive impact on the world and those around me.

# ABSTRACT OF THE THESIS

Cellular Crosslinking of *B. subtilis* via Conjugation of Polymerizable Handles

by

Wesley Alan Groves

Master of Science in Biomedical Engineering

University of California, Irvine, 2022

Professor Seunghyun Sim, Chair

The intersection of materials science and synthetic biology enables the production of engineered living materials (ELMs) with functionalities such as the ability to self-repair, autonomously control morphology, and sense-and-respond to environmental stimuli. The interface between living cells and synthetic polymer scaffolds is a crucial design element of ELMs that requires further research to make these materials industrially relevant. Herein, we report the development of two unique conjugation strategies that enable covalent crosslinking of *B. subtilis* within a PEGDA hydrogel. *B. subtilis* surface chemistry is exploited to conjugate polymerizable "handles" that enable cellular crosslinking via free radical polymerization.

# BACKGROUND AND INTRODUCTION

Biological materials found in the natural world such as skin, wood, or bacterial biofilms are capable of extraordinary functions including the ability to self-assemble, sense-and-respond to environmental stimuli, and self-repair [1, 2]. These functions are made possible by the living cells within the material, governed by a genetic code that enables them to sense their surroundings and change their behavior accordingly. The cellular components synthesize these scaffolds from raw building blocks and can control material morphology with precision across numerous length scales [1, 3]. Evolution has produced a vast array of unique material functions such as enhanced electrical conductivity, underwater adhesion, and the ability to change colors [1,3,4]. The autonomous, complex, and functional nature of living materials serves as a key inspiration in the field of materials science.

Advancement in the field of synthetic biology has enabled researchers to engineer the genetic code of host organisms to synthesize recombinant proteins. Yeast and bacterial cells are frequently engineered to synthesize biofuels and therapeutics or even perform complicated multi-step reaction cascades [5,6]. The overlap of synthetic biology and materials science disciplines has given birth to the field of engineered living materials (ELM). There have been two main approaches to designing ELMs; top-down design where living cells are encapsulated in a synthetic scaffold, or bottom-up design where cells are engineered to synthesize, secrete, and maintain their own matrix [3]. The bottom-up approach enables researchers to target the nanoscale architecture of the material, building higher-order structures by genetic engineering of the host organism [7]. An excellent example of a bottom-up approach comes from Huang et al. who have engineered gram-positive *B. subtilis* to secrete a recombinant amyloid protein to display a variety of reactive protein handles throughout a bacterial biofilm [6]. However, bottom-up approaches are difficult to

control at larger length scales which is why many researchers are adopting a top-down approach to manufacture ELMs at the centimeter to meter length scale. Additionally, the top-down approach enables commonly used manufacturing methods such as cast-molding or additive manufacturing (i.e. 3D printing) [7]. An example of the top-down approach is demonstrated by Chan et al. who encapsulated fibroblast cells within a PEGDA scaffold to create a 3D printable bio-ink with precise control over cell distribution [8]. Each approach has its advantages; therefore, it is necessary to consider desired material specifications before determining the appropriate design approach.

Another consideration when designing an ELM is the selection of a suitable host organism. For many, bacterium is the ideal host organism as they possess profound metabolic diversity making them capable of synthesizing a wide variety of functional proteins [9]. Particularly, *B. subtilis* is a commonly used organism in the industrial production of a variety of enzymes due to their extraordinary capacity to secrete proteins in culture medium [10]. *B. subtilis* can also sporulate under harsh conditions, including dehydration. As such, they can be desiccated, stored, transported, and can be rehydrated on demand [11]. Lastly, *B. subtilis* is genetically tractable and is generally recognized as safe (GRAS) by the US Food and Drug Administration (FDA), making it the ideal host organism for many ELM applications.

The number of publications released in the field of ELM is increasing rapidly [12]. However, there are some fundamental barriers preventing these materials from being immediately useful for suggested applications. The most prominent barrier is the need for a robust biocontainment strategy. While ELMs may be useful in a wide variety of situations, we certainly do not want to inadvertently release genetically modified organisms (GMOs) to disrupt local ecosystems. Therefore, a few prior studies explore novel biocontainment methods, including the method relies on genetic circuitry and specialized chemistry within the material matrix [13]. Some

researchers are utilizing genetic circuits that prevent self-replication or using auxotrophic host organisms; however, neither of these strategies are viable solutions for sustaining material function in the long-term [13]. For these to maintain function long-term, the host organisms must receive a continuous supply of the inducer or auxotrophic growth factor – which is simply not possible in some applications [13]. Others such as Guo et al. are cleverly utilizing *E. coli* engineered to express adhesin proteins on their membrane surface, conjugating the cells to the surrounding dextran scaffold [14]. However, this strategy introduces a metabolic burden onto the cells thus providing an evolutionary incentive to deactivate the containment system [13]. There is an evident need for more robust, long-term, and effective engineered biocontainment strategies.

Herein we describe a top-down approach to designing a 3D printable bio-ink that covalently cross-links cells within a hydrogel matrix. **We exploit *B. subtilis* surface chemistry to conjugate polymerizable handles to the surface of both vegetative cells and spores using two distinct conjugation methods.** The cells are then encapsulated and crosslinked into a polyethylene glycol diacrylate (PEGDA) scaffold using photopolymerization. The 3D printable hydrogel design, *in situ* cell viability, and mechanical characterization of the ELM are reported within this body of work.

# Chapter 1: Determination and characterization of hydrogel components

## 1.1 Motivation and rationale

Design of the synthetic scaffold requires several components; a polymeric crosslinker, a shear-thinning element to enable 3D printability, a photo initiator to facilitate free radical polymerization, and a cell to serve as the functional bioreactor. Polyethylene glycol diacrylate (PEGDA) was used as the crosslinker because of its commercial availability and can be acquired in a variety of molecular weights. Lithium phenyl-2,4,6-trimethylbenzoylphosphinate (LAP) was used as photo initiator. Xanthan was used as a shear-thinning element because it is biocompatible and only requires a small amount to impart a strong shear-thinning effect. Lastly, PY79 *B. subtilis* was chosen as a host organism because it is generally regarded as safe, genetically tractable, capable of secreting a wide variety of functional recombinant proteins, and capable of forming spores under harsh conditions [11]. It is necessary to characterize each component of the synthetic scaffold as to how it contributes to the overall properties of the bio-ink.

## 1.2 Rheological characterization and test printing

Firstly, the optimal xanthan concentration was determined through rheological characterization and test printing. Four xanthan concentrations varying from 0.5%–2% w/v in PBS were characterized using a flow ramp analysis on an HR-2 hybrid rheometer to investigate their shear thinning behavior (Figure 1). To evaluate print fidelity, the varying xanthan percentages were 3D printed using an Allevi 2 bioprinter. It was qualitatively determined that the 1.5% w/v solution had the best print fidelity, thus all subsequent hydrogel mixtures were fixed with this concentration of xanthan.

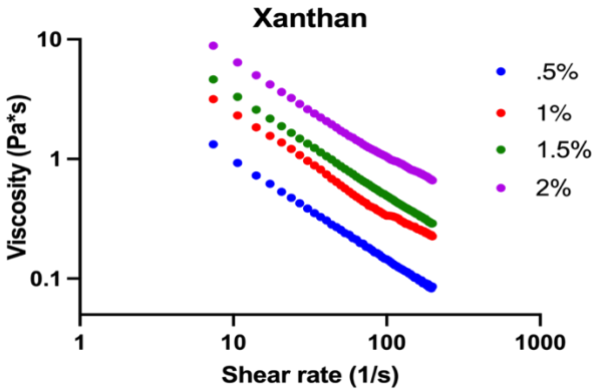


*Figure 1: Rheological flow-ramp analysis of varying xanthan concentrations using HR-2 hybrid rheometer and a 25-mm parallel plate.*

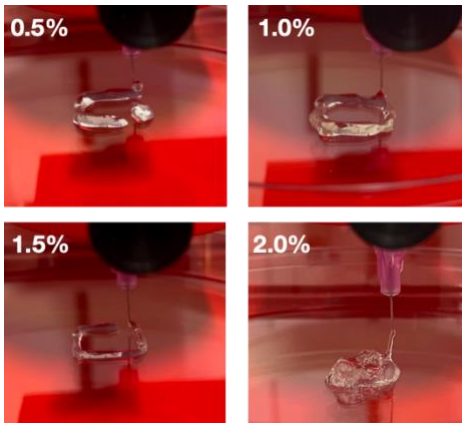


*Figure 2: Test prints of 0.5% (top left), 1.0%, 1.5%, and 2.0% w/v xanthan (bottom right). It was determined that 1.5% w/v xanthan had the best print fidelity.*

A range of PEGDA molecular weights were used to vary parameters such as cross-linking density and pore size within the polymeric network. To better understand the contribution of PEGDA to the mechanical properties of the material, polymerized PEGDA 4 kDa, 10 kDa, and 20 kDa hydrogels were characterized using a strain-ramp protocol on an HR-2 hybrid rheometer (Figure 3). The samples were prepared by dissolving PEGDA in PBS at 10% w/v, adding xanthan to 1.5% w/v adding LAP photo-initiator to 5mM, and photocuring in cast-mold using a 405nm LED bulb. Supply-chain issues prevented reliable acquisition of data using PEGDA 10 kDa, thus all subsequent analyses included only 4 kDa and 20 kDa PEGDA crosslinkers held constant at 10% w/v.

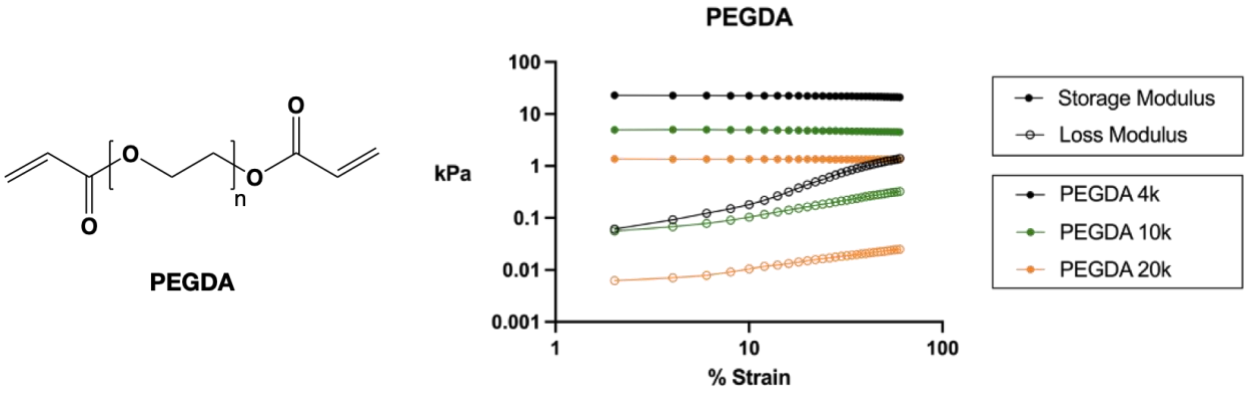


*Figure 3: Molecular structure of PEGDA crosslinker (left) and strain-ramp rheological analysis of 10% w/v PEGDA molecular weights 4 kDa, 10kDa, and 20kDa (right).*

## Chapter 2: Evaluation of conjugation strategy, cell viability, and cell growth

### 2.1: N-Hydroxysuccinimide (NHS) coupling of polymerizable methacrylate handle

Our strategy exploits the surface chemistry of *B. subtilis* cells and spores to conjugate polymerizable moieties to the outer peptidoglycan cell wall or protein crust so that the living entities may be crosslinked through free radical polymerization. The first of two conjugation methods involves NHS amine coupling, a commonly used strategy in the field of nanotechnology [15]. The objective is to use NHS-methacrylate to react with free amines present on the peptidoglycan cell wall in vegetative *B. subtilis* cells and on the outer spore crust in *B. subtilis* spores [16]. The general reaction scheme can be found in Figure 4 below. A sulfo-cy5 NHS ester fluorescent probe was used to visualize the availability of this molecular target on both *B. subtilis* cells and spores (Figure 5).

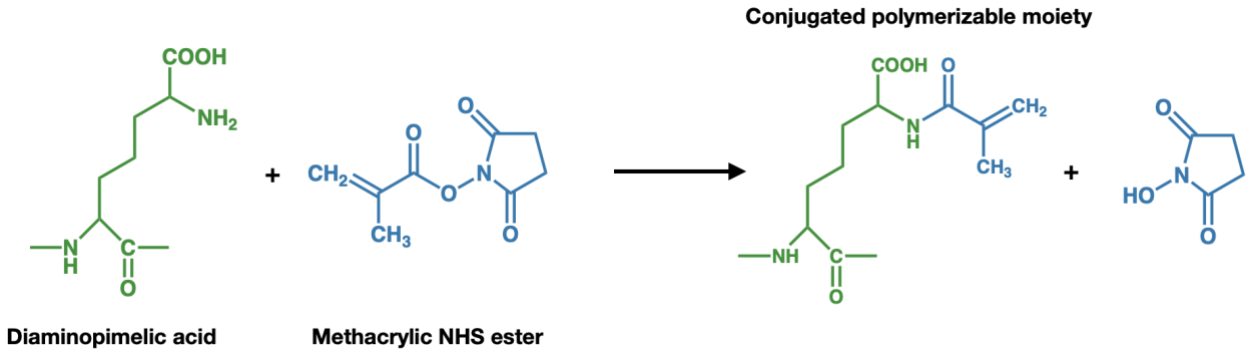


*Figure 4: Conjugation scheme of NHS methacrylate with diaminopimelic acid (DAP) residues present on B. subtilis cell wall. The product is a polymerizable methacrylate handle installed on the cell surface.*

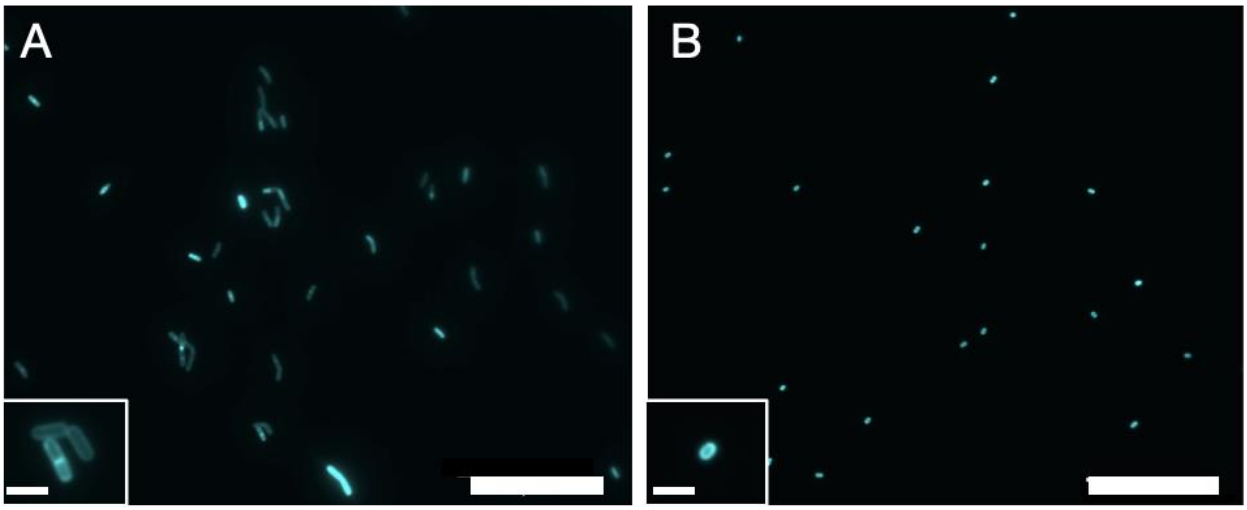


*Figure 5: Microscope images confirming the presence of molecular targets on B. subtilis surface. A) Vegetative B. subtilis cell stained with Sulfo-Cy5 NHS ester. B) B. subtilis spore stained with Sulfo-Cy5 NHS ester. Scale bars: 30 μm. Inset scale bars: 3 μm*

## 2.2: Phenyl-boronic acid (PBA) coupling of polymerizable acrylate handle

The second conjugation strategy utilizes boronic acid-diol chemistry to target cis-diols present on teichoic acid residues in *B. subtilis* peptidoglycan [17]. This reaction results in a dynamic covalent bond that is robust yet reversible. In a recent publication from the Sim lab, the utility of this bond in constructing cell-material interface for dynamic living materials has been demonstrated [17]. These qualities also enabled biocontainment of *B. subtilis* cells over 96 hours

in a nutrient-rich condition. The conjugation scheme is shown below in Figure 6. To visualize the location of cis-diol moieties on *B. subtilis* and *B. subtilis* spore surfaces, cells were imaged with APBA-sulfo-cy5 fluorescent dye (Figure 7, credit: Hyuna Jo).

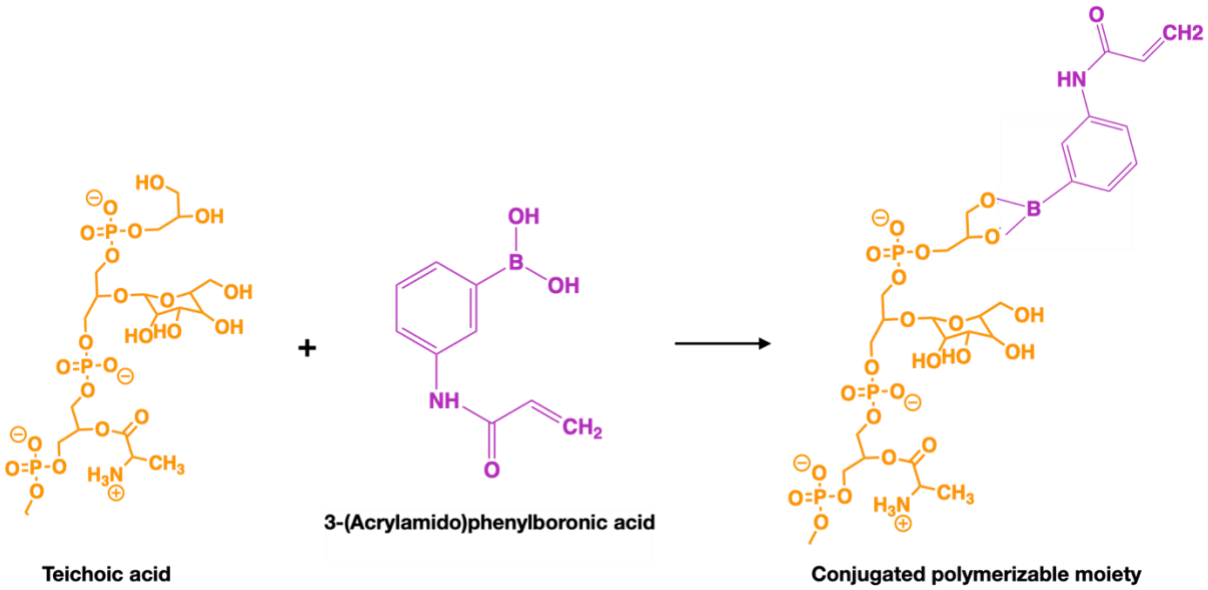


*Figure 6: Reaction scheme of 3-(acrylamido)phenylboronic acid conjugating to teichoic acid residues found on B. subtilis cell and spore surfaces.*

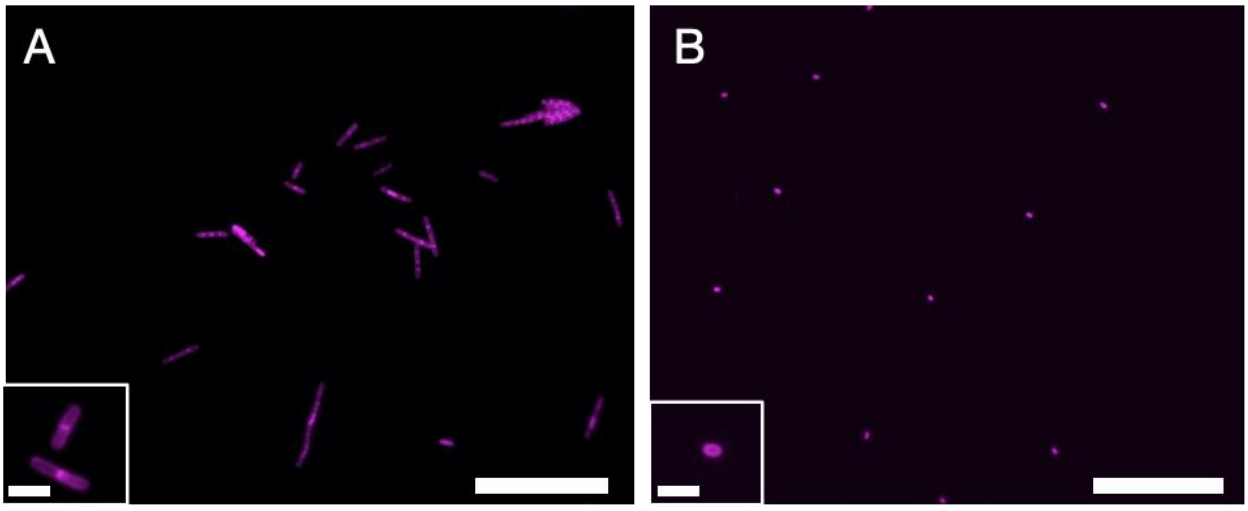


*Figure 7: Microscope images confirming the presence of molecular targets on B. Subtilis surface. A) Vegetative B. subtilis cell stained with Sulfo-Cy5 phenyl-boronic acid. Credit: Hyuna Jo, PhD. B) B. subtilis spore stained with Sulfo-Cy5 phenyl-boronic acid. Credit: Hyuna Jo, PhD. Scale bars: 30μm. Inset scale bars: 3μm*

### 2.3 Analysis of cell viability and growth *in situ*

To effectively crosslink *B. subtilis* in a PEGDA matrix using the aforementioned conjugation strategies, the cells must be able to survive a free-radical polymerization reaction. Vegetative *B. subtilis* cells were first reacted with 15 mM methacrylic acid NHS ester in PBS at room temperature for one hour under shaking conditions. Conjugated cells were added to the pre-polymerization hydrogel mixture (10% w/v PEGDA, 1.5% w/v xanthan, and 5 mM LAP in PBS), exposed to photopolymerization, stained with a fluorescent viability stain (SYTO9 and propidium iodide), and imaged using confocal microscopy. A representative image of cellular viability is found below in Figure 8. It was observed that most of the cells remained alive (fluorescing green) after exposed to the reaction conditions. Furthermore, the cells were oriented in fibril clusters of 2-4 cells in length, indicating they are even capable of dividing *in situ*.

One of the key advantages of using *B. subtilis* as a host organism is the ability to sporulate and germinate on demand. To investigate this behavior, we employed a strain of *B. subtilis* engineered to display the fluorophore mWasabi in its spore coat and intracellular red fluorescent protein (RFP) in its vegetative state [17]. This gives *B. subtilis* two distinct fluorescent markers that enable the differentiation between sporulated and vegetative states. Spores of this dual-fluorescent *B. subtilis* were infused into the pre-polymerized hydrogel mixture and subsequently encapsulated through photocuring. The hydrogels were submerged in LB medium and fluorescent images were taken at various timepoints to visualize germination and eventual colonization (Figure 9).

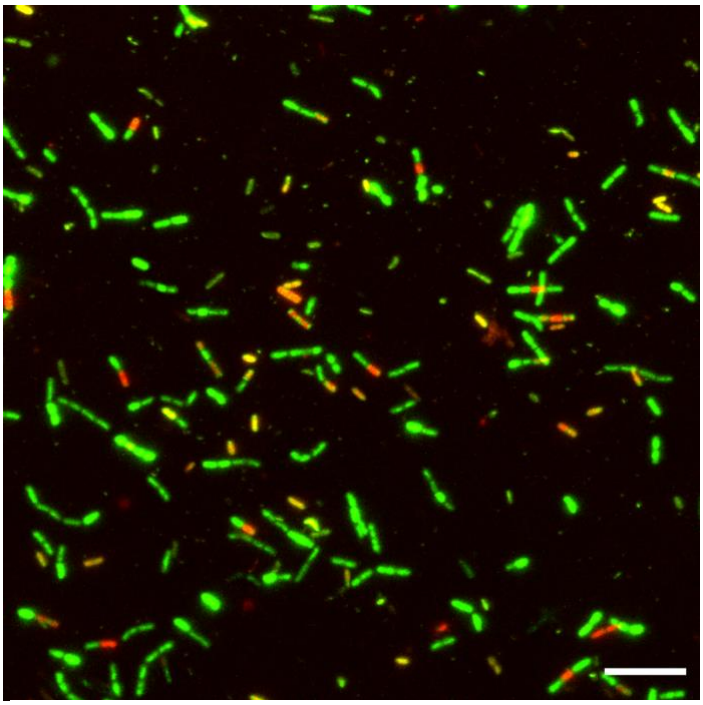

*Figure 8: Confocal microscope image of B. subtilis conjugated with NHS methacrylate and polymerized in PEGDA 4 kDa and subsequently stained with SYTO9 and propidium iodide. Green and red represent live and dead cells respectively. Imaged at 100x. Scale bar: 10 μm*

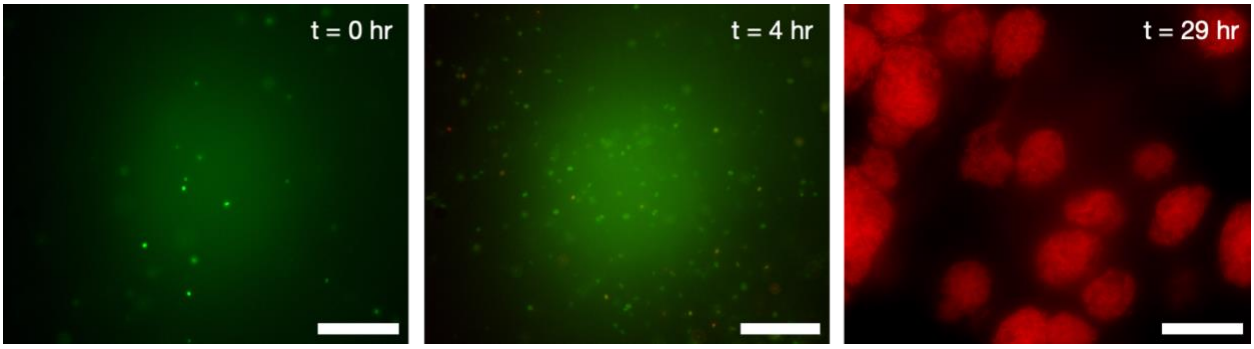


*Figure 9: Images of dual-fluorescent B. subtilis within a polymerized hydrogel. DF B. subtilis cells were engineered to express mWasabi in their spore coat and express intracellular RFP in their vegetative state [17]. Scale bars: 30 μm*

# Chapter 3: Mechanical characterization of engineered living material (ELM)

## 3.1 Mechanical characterization strategies

On the basis of the experiments with fluorescent probes confirming the presence of molecular targets on the cell surface, we set out to investigate whether the cells/spores would be crosslinked with polymeric scaffold of hydrogels. The parameter to be investigated is the cross-linking density which is positively correlated with material stiffness [18]. For this study, *B. subtilis* spores were used as their concentration within the hydrogel is held constant.

A reliable mechanical characterization technique employed in this study is rheological analysis. Through rheology, the storage (G') and loss (G'') moduli, which describe the material's viscoelastic behavior, are obtained. The storage modulus (G') describes the energy stored in the elastic framework of a viscoelastic material and can characterize material elasticity [19]. The loss modulus (G'') describes the energy dissipated through molecular rearrangement in a viscoelastic material and can characterize material viscous behavior [19]. For this study, we used an HR-2 hybrid rheometer with an 8-mm parallel plate to characterize the spore-laden PEGDA hydrogels. We hypothesized that successful cellular crosslinking would increase the overall crosslinking density which can be demonstrated by an increase in materials' storage modulus (G').

An emerging strategy for mechanical characterization is nanoindentation testing. This requires a highly sensitive probe with known stiffness to indent the material. The probe deflection and indentation depth are used to calculate the material's Young's modulus. A Piuma nanoindenter (Optics 11 Life) was employed for this study. We hypothesized that successful spore crosslinking will increase average crosslinking density throughout the material which can be inferred by an increased Young's modulus.

### 3.2 NHS Conjugation

Spores were conjugated with methacrylate NHS ester at 15mM for 1 hour under shaking conditions (reaction scheme in Figure 4). Conjugated spores were infused into pre-polymerized PEGDA solutions (10% w/v PEGDA, 1.5% w/v xanthan, and 5mM LAP in PBS) and subsequently polymerized via photocuring using a 405nm LED bulb. The hydrogels were then analyzed using an HR-2 hybrid rheometer with an 8-mm parallel plate (Figure 10). The observed trend was inverse of our proposed hypothesis in that the NHS-conjugated spore laden hydrogels had reduced storage moduli G'. The trend observed through rheological analysis was also seen in the indentation studies where the NHS samples had reduced effective Young's moduli (Figure 11). This trend was replicated across 3 experimental replicates and was related to the concentration of methacrylate NHS ester. As the concentration methacrylate NHS ester was increased, the trend was exacerbated further, reducing material stiffness so much that the material could barely be handled without deteriorating.

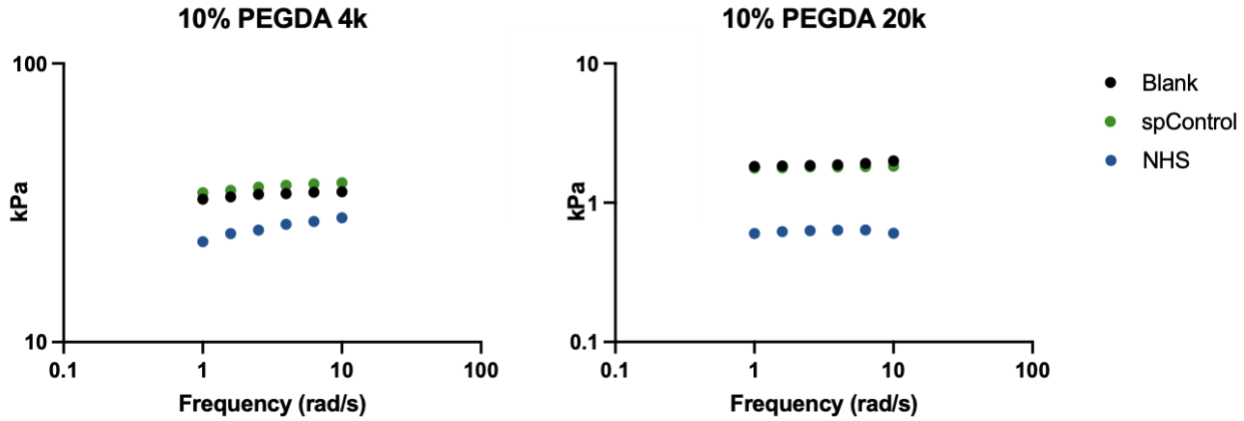


*Figure 10: Storage moduli (G') of B. subtilis spore laden PEGDA hydrogels. Blank gels did not contain spores, spControl gels contain spores with no conjugation, NHS gels contained spored conjugated with methacrylate NHS ester.*

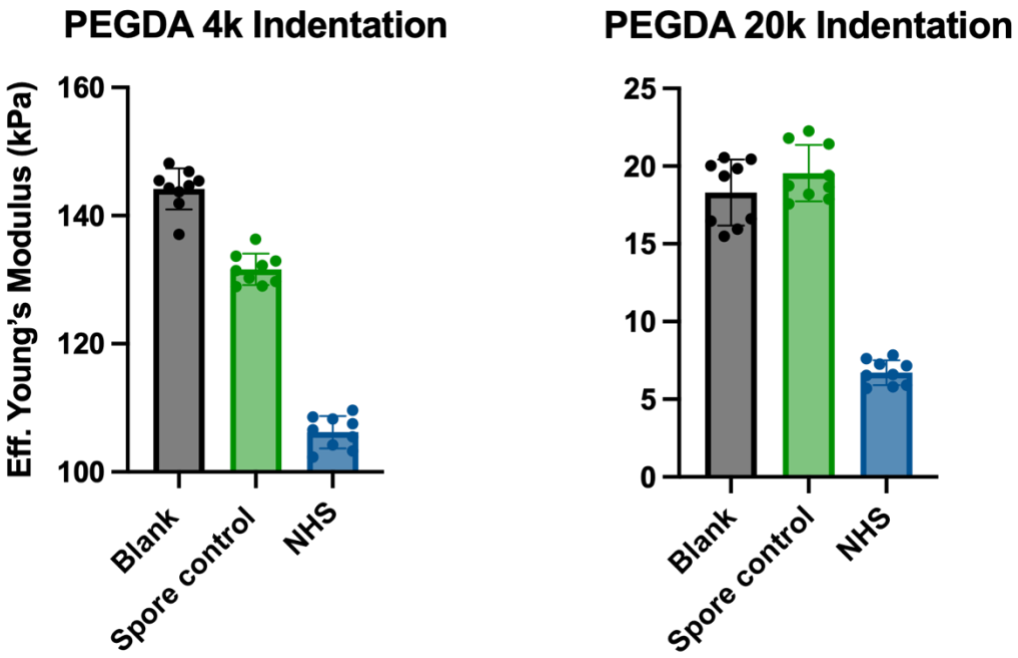


*Figure 11: Indentation-based characterization of B. subtilis spore laden PEGDA hydrogels. Blank gels contain no spores, spore control gels contain spores with no conjugation, and NHS gels contain spores conjugated with methacrylate NHS ester. Each point is representative of an indentation measurement within the same sample.*

### 3.3 PBA Conjugation

*B. subtilis* spores (OD = 1) were reacted with 3-(acrylamido)phenylboronic acid at 15mM for 1 hour under shaking conditions and subsequently infused into a pre-polymerized PEGDA hydrogel mixture (10% w/v PEGDA, 1.5% w/v xanthan, and 5mM LAP in PBS). The hydrogels were then photocured and allowed to fully swell overnight in PBS. Rheological and indentation characterization were used with the hypothesis being that successful spore crosslinking would result in increased storage and elastic moduli.

Rheological analysis demonstrated no noticeable difference in the 4 kDa molecular weight PEGDA hydrogels, however, there was a replicable trend shown in 20 kDa PEGDA. The phenylboronic acid (PBA) hydrogels consistently had higher storage moduli, indicating an

increased crosslinking density. This trend was also observed in the indentation analysis (Figure 13), with a more dramatic increase in elastic modulus for PBA-conjugated spores in the 20k PEGDA hydrogels. This indicates that the PBA conjugation strategy is successfully crosslinking spores and that they are physically contributing to material elastic properties.

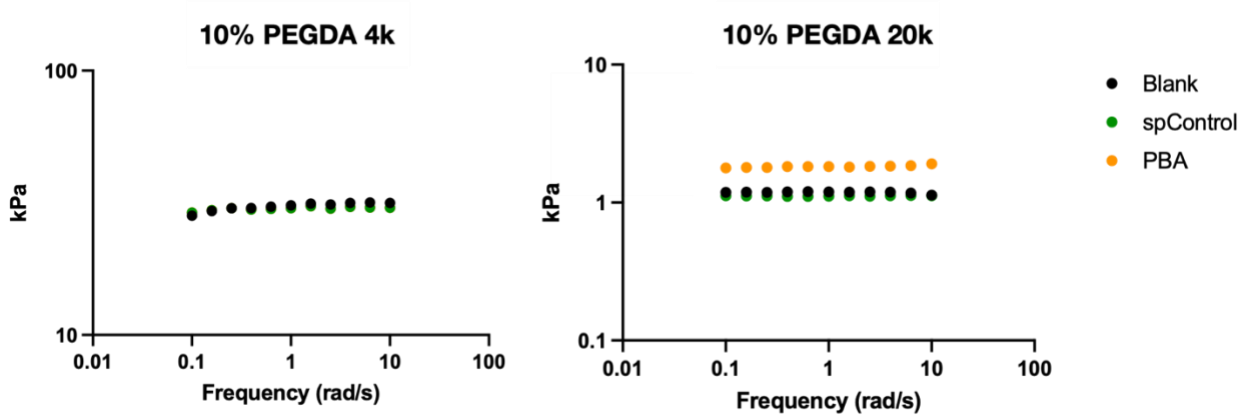


*Figure 12: Storage moduli (G') of B. subtilis spore laden PEGDA hydrogels. Blank gels did not contain spores, spControl gels contained spores with no conjugation, PBA gels contained spores conjugated with 3-(acrylamido)phenylboronic acid.*

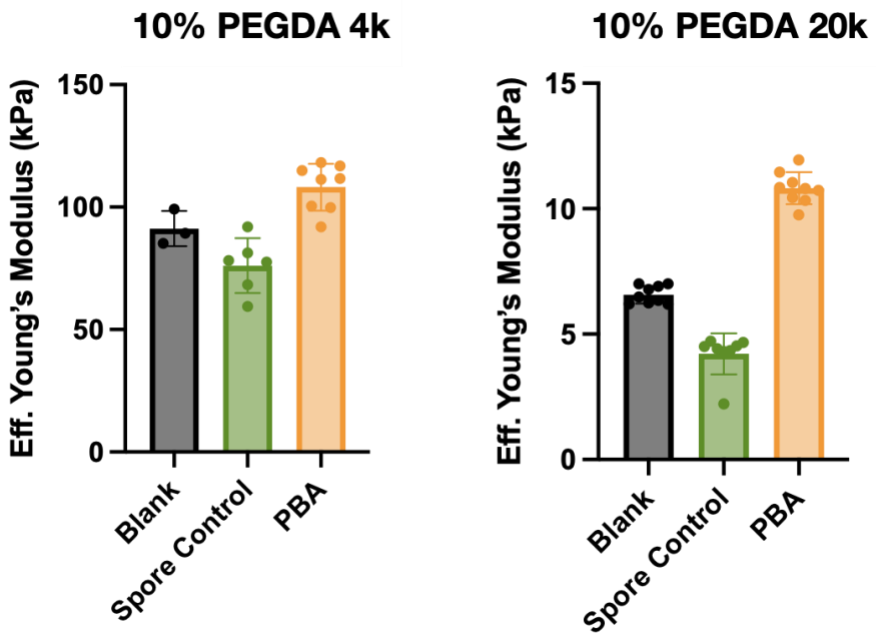


*Figure 13: Indentation-based characterization of B. subtilis spore laden PEGDA hydrogels. Blank gels contain no spores, spore control gels contain spores with nc conjugation, and PBA gels contain spores conjugated with 3(acrylamido)phenylboronic acid. Each point is representative of an indentation measurement within the same sample.*

## DISCUSSION AND CONCLUSION

The novelty of this work is rooted in the strategy of using conjugation strategies to implant polymerizable molecular "handles" on the surface of cells so that they may be covalently crosslinked in engineered living materials. The work reported in chapters 1 and 2 above demonstrate that *B. subtilis* is capable of surviving and proliferating within these materials. Through mechanical characterization, a few puzzling trends were observed which require further discussion.

Through rheological and indentation-based analyses, we found that the NHS conjugation reduced material stiffness while the PBA strategy increased stiffness. We believe that this is due to molecular differences in the polymerizable motifs on the two conjugant molecules. Specifically, methacrylate NHS ester forms tertiary carbon radicals whereas 3-(acrylamido)phenylboronic acid forms secondary carbon radicals when undergoing polymerization. Since tertiary radicals are more stable, this likely results in different polymerization reaction rates leading to preferential addition onto the growing PEGDA chain [20]. The increased stability of methacrylate NHS ester's tertiary radicals could also lead to premature termination of the polymer chain, which could explain the reduced stiffness present in NHS-

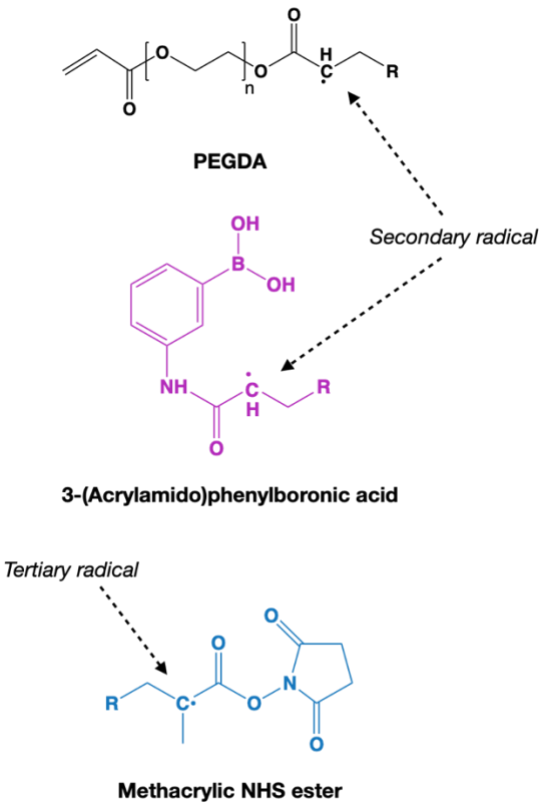


*Figure 14: Molecular structure and radical positioning of PEGDA (secondary radical), 3-(acrylamido)phenylboronic acid (secondary radical) and methacrylic NHS ester (tertiary radical).*

conjugated PEGDA hydrogels. The NHS conjugation strategy still has potential; however, a new conjugant molecule should be synthesized to avoid the potential of preferential addition.

Mechanical analyses demonstrated an increase in mechanical stiffness within hydrogels containing spores conjugated with 3-(acrylamido)phenylboronic acid only within the 20 kDa molecular weight PEGDA samples. We speculate that the crosslinking density within 4 kDa PEGDA is not substantially different from that of 4 kDa PEGDA scaffold with cross-linked cells. We predict that this trend would become more dramatic as PEGDA molecular weight is increased.

The discoveries made in this body of work paves a path for future studies. We confirmed the presence and availability of two molecular targets on the surface of *B. subtilis* cells and spores. Additionally, we have shown that *B. subtilis* can survive and proliferate within a synthetic hydrogel scaffold after undergoing free radical polymerization. Future studies should test the capacity for biocontainment which would make cell-laden materials deployable in the real world. Additionally, the incorporation of engineered *B. subtilis* could demonstrate further utility of this material design, including the ability to interact and modify the polymer matrix. Lastly, expanding to other host organisms, including plant or animal cells, will further increase the number of functions this engineered living material can offer to infrastructure, medicine, and the environment.

# METHODS

## Bacterial Growth Conditions

*B. subtilis* cultures were grown by inoculating a single colony in Lysogeny broth (LB) medium at 37 °C for 16-hr in a shaker-incubator. Dual-fluorescent *B. subtilis* strains were grown in LB medium supplemented with 5 $\mu$g/mL chloramphenicol.

## *B. subtilis* sporulation

*B. subtilis* cultures were inoculated in LB medium and allowed to grow to mid-exponential phase (~4 hours). The cell solution was centrifuged at 5000 rpm for 10 minutes, the supernatant aspirated, and cells resuspended in Sterilini & Mandelsten (S&M) medium. Cells underwent sporulation while suspended in S&M medium for 16 hours. Solution was centrifuged at 5000 rpm for 10 minutes then the supernatant was aspirated. The pellet was resuspended in 50 $\mu$g/mL lysozyme solution to lyse any non-sporulated cells. After 30 minutes, cells were centrifuged, resuspended in PBS, and stored in 4 °C until use.

## Fluorescent imaging of sulfo-cy5 NHS ester conjugated cells

Prepared cells and spores were suspended to an $OD_{600}$ of 1 and underwent three PBS washes to remove remaining LB medium. The cell solutions were then resuspended in PBS and stained with sulfo-cy5 NHS ester at 0.1 mg/mL for 10 minutes, being shaken at 30rpm on a rotary shaker. Three more PBS washes were performed to remove excess stain prior to fluorescent imaging using a 630 nm excitation wavelength and a peak emission of 670 nm.

**Fluorescent imaging of APBA sulfo-cy5 conjugated cells**

Prepared cells and spores were suspended to an $OD_{600}$ of 1 and underwent three PBS washes to remove the remaining LB medium. The cell solutions were then resuspended in PBS and stained with APBA-sulfo-cy5 at 15 µM at 25 °C for 3 hours, being shaken throughout. Three more PBS washes were performed to remove excess stain prior to fluorescent imaging using a 630 nm excitation wavelength. [17]

**Methacrylate NHS ester conjugation of spores**

1 M stock solution of methacrylate NHS ester dissolved in DMSO was added to cell or spore solutions (OD = 1) to a final reaction concentration of 15 mM for 1 hr at room temperature, being shaken throughout.

**3-(Acrylamido)phenylboronic acid conjugation of spores**

0.75 M stock solution of 3-(acrylamido)phenylboronic acid dissolved in DMSO was added to cell or spore solutions (OD = 1) to a final reaction concentration of 15 mM for 1-hr at room temperature, being shaken throughout.

**Preparation of and polymerization of PEGDA hydrogels**

Polyethylene glycol diacrylate (PEGDA) was added to PBS solutions to 10% w/v. Xanthan was then added to 1.5% w/v. The solutions were then vortexed for 1 minute to distribute the xanthan. The solutions were stored at 4 °C for more than 24 hours to allow xanthan to fully swell and distribute evenly. Spores, either treated or untreated, were then infused into the PEGDA solution and thoroughly mixed. Lastly, 250 mM stock solution of LAP photo-initiator was added to achieve a final concentration of 5 mM and mixed thoroughly. The solutions were centrifuged to remove

any air bubbles. The pre-polymerized hydrogel solutions were pipetted into a circular mold with a radius of 8-mm and a height of 0.5-mm. A glass slide was placed over the mold, ensuring no air bubbles are introduced. Using a ThorLabs 405 nm LED bulb (irradiance = 0.209 W/cm$^2$), the hydrogels were photocured for 5 minutes. The polymerized hydrogels were placed into a PBS solution where they were allowed to fully swell overnight (>12 hours).

**3D printing of xanthan solutions**

Xanthan solutions of various concentrations were added to syringes compatible with the Allevi 2 bioprinter. Solutions were printed into a cube geometry using a 30-guage extrusion needle at 15 psi.

**Rheological Characterization of Hydrogel**

Materials were analyzed using an HR-2 hybrid rheometer from TA Instruments. Xanthan solutions were tested through a flow-ramp protocol (2-200Hz) using a 25-mm parallel plate. Polymerized hydrogels were tested using a frequency-ramp protocol with an 8-mm parallel plate. This protocol set applied strain constant at 0.2% and varied oscillation frequency from 1 to 10 Hz. Sample slipping was observed beyond 10 Hz, regardless of applied axial force.

**Indentation Characterization of Hydrogel**

Indentation analysis was performed using a Piuma Nanoindenter from Optics11 Life using a probe with a stiffness of 0.29 N/m and radius of 8.5 $\mu$m. Prepared samples were adhered to a glass slide using Gorilla Glue and then submerged in a PBS solution for indentation. A matrix scan was used to take a total of 9 indentations per sample at an indentation depth of 4 $\mu$m. Effective Young's modulus values were calculated from the resultant force-indentation data using a Hertzian model [21].

**References:**


[1] C. Gilbert and T. Ellis, "Biological engineered living materials: Growing functional materials with genetically programmable properties," *ACS Synthetic Biology*, vol. 8, no. 1, pp. 1–15, 2018.

[2] P. Q. Nguyen, N.-M. D. Courchesne, A. Duraj-Thatte, P. Praveschotinunt, and N. S. Joshi, "Engineered living materials: Prospects and challenges for using biological systems to direct the Assembly of Smart Materials," *Advanced Materials*, vol. 30, no. 19, p. 1704847, 2018.

[3] A. Rodrigo-Navarro, S. Sankaran, M. J. Dalby, A. del Campo, and M. Salmeron-Sanchez, "Engineered living biomaterials," *Nature Reviews Materials*, vol. 6, no. 12, pp. 1175–1190, 2021.

[4] M. D. Ramirez and T. H. Oakley, "Eye-independent, light-activated chromatophore expansion (LACE) and expression of phototransduction genes in the skin of *octopus bimaculoides*," *Journal of Experimental Biology*, vol. 218, no. 10, pp. 1513–1520, 2015.

[5] A. S. Khalil and J. J. Collins, "Synthetic Biology: Applications come of age," *Nature Reviews Genetics*, vol. 11, no. 5, pp. 367–379, 2010.

[6] J. Huang, S. Liu, C. Zhang, X. Wang, J. Pu, F. Ba, S. Xue, H. Ye, T. Zhao, K. Li, Y. Wang, J. Zhang, L. Wang, C. Fan, T. K. Lu, and C. Zhong, "Programmable and printable bacillus subtilis biofilms as engineered living materials," *Nature Chemical Biology*, vol. 15, no. 1, pp. 34–41, 2018.

[7] W. V. Srubar, "Engineered living materials: Taxonomies and emerging trends," *Trends in Biotechnology*, vol. 39, no. 6, pp. 574–583, 2021.

[8] V. Chan, P. Zorlutuna, J. H. Jeong, H. Kong, and R. Bashir, "Three-dimensional photopatterning of hydrogels using stereolithography for long-term cell encapsulation," *Lab on a Chip*, vol. 10, no. 16, p. 2062, 2010.

[9] J. J. Hug, D. Krug, and R. Müller, "Bacteria as genetically programmable producers of bioactive natural products," *Nature Reviews Chemistry*, vol. 4, no. 4, pp. 172–193, 2020.

[10] J. M. van Dijl and M. Hecker, "Bacillus subtilis: From soil bacterium to super-secreting cell factory," *Microbial Cell Factories*, vol. 12, no. 1, p. 3, 2013.

[11] D. Higgins and J. Dworkin, "Recent progress in *bacillus subtilis* sporulation," *FEMS Microbiology Reviews*, vol. 36, no. 1, pp. 131–148, 2012.

[12] L. Xu, X. Wang, F. Sun, Y. Cao, C. Zhong, and W.-B. Zhang, "Harnessing proteins for engineered living materials," *Current Opinion in Solid State and Materials Science*, vol. 25, no. 1, p. 100896, 2021.

[13] J. W. Lee, C. T. Chan, S. Slomovic, and J. J. Collins, "Next-generation biocontainment systems for engineered organisms," *Nature Chemical Biology*, vol. 14, no. 6, pp. 530–537, 2018.

[14] S. Guo, E. Dubuc, Y. Rave, M. P. A. Verhagen, S. A. E. Twisk, T. van der Hek, G. J. M. Oerlemans, M. C. M. van den Oetelaar, L. S. van Hazendonk, M. Brüls, B. V. Eijkens, P. L. Joostens, S. R. Keij, W. Xing, M. Nijs, J. Stalpers, M. Sharma, M. Gerth, R. J. E. A. Boonen, K. Verduin, M. Merkx, I. K. Voets, and T. F. A. de Greef, "Engineered living materials based on adhesin-mediated trapping of programmable cells," *ACS Synthetic Biology*, Feb. 2020.

[15] K. E. Sapsford, W. R. Algar, L. Berti, K. B. Gemmill, B. J. Casey, E. Oh, M. H. Stewart, and I. L. Medintz, "Functionalizing nanoparticles with biological molecules: Developing chemistries that facilitate nanotechnology," *Chemical Reviews*, vol. 113, no. 3, pp. 1904–2074, 2013.

[16] D. M. Angeles and D.-J. Scheffers, "The cell wall of bacillus subtilis," *Bacillus: Cellular and Molecular Biology (Third edition)*, 2017.

[17] H. Jo and S. Sim, "Programmable living materials constructed with dynamic covalent interface between synthetic polymers and B. subtilis," *ACS Applied Materials & Interfaces*, vol. 14, no. 18, pp. 20729–20738, 2022.

[18] L. Pescosolido, L. Feruglio, R. Farra, S. Fiorentino, I. Colombo, T. Coviello, P. Matricardi, W. E. Hennink, T. Vermonden, and M. Grassi, "Mesh size distribution determination of interpenetrating polymer network hydrogels," *Soft Matter*, vol. 8, no. 29, p. 7708, 2012.

[19] H. M. Wyss, "Rheology of soft materials," *Fluids, Colloids and Soft Materials: An Introduction to Soft Matter Physics*, pp. 149–164, 2016.

[20] Y. Reyes and J. M. Asua, "Revisiting chain transfer to polymer and branching in controlled radical polymerization of butyl acrylate," *Macromolecular Rapid Communications*, vol. 32, no. 1, pp. 63–67, 2010.

[21] D. C. Lin, D. I. Shreiber, E. K. Dimitriadis, and F. Horkay, "Spherical indentation of soft matter beyond the Hertzian regime: Numerical and experimental validation of hyperelastic models," *Biomechanics and Modeling in Mechanobiology*, vol. 8, no. 5, pp. 345–358, 2008.